An equivalent single layer shear deformation plate theory with superposed shape functions for laminated composite plates

M. AYDOGDU

Department of Mechanical Engineering, Trakya University, 22030, Edirne, Turkey,
e-mail: metina@trakya.edu.tr

A single layer shear deformation plate theory with superposed shape functions for laminated composite plates has been proposed. Some of the previously developed, five degrees of freedom shear deformation theories, including parabolic [1], hyperbolic [2], exponential [3] and trigonometric [4] plate theories have been superposed by applying different theories in the different in- plane directions of the composite plate. Statics and dynamics of composite plate problems have been investigated. It was obtained that using different shape functions in the different in-plane directions may decrease the percentage error of stress and deflection. Present hyperbolic-exponential and parabolic-exponential theories predict stiffer properties (give lower bending and stress values, and higher frequency, and buckling loads when compared to the 3-D elasticity). Some improvements were determined for y-z component of the transverse shear stress using hyperbolic-exponential and parabolic-exponential theories for symmetric cross-ply composite plates when compared to available single shape function plate models. Global behaviours (vibration frequency and critical buckling loads) are predicted within %5 accuracy similar to plate theories with single shape functions.

Key words: laminated composites, shear deformation plate theory, bending, vibration, buckling.

1. Introduction

Laminated composite structures are preferred in many areas like aerospace, automotive and submarine applications due to their low specific density and low specific modulus. These structures are used generally in rod, beam, plate and shell forms depending on the needs. It is well known that basically two different approaches are used in the modelling of laminated composite structures: single layer theories and discrete layer theories. In the latter group, the number of variables depends on the number of layers in the composite structure, so it is relatively difficult to use them when modelling composite structures. Moreover, in the former group, the whole laminated structure is considered as an equivalent single layer in the analysis.

Displacement based single layer theories can be divided into two groups: The classical laminated plate theory and shear deformation plate theories. In the

classical plate theory, a plane stress assumption is assumed for the deformation, whereas transverse shear deformations are also included in the shear deformation theories using different transverse shear strain assumptions. It was shown in the many of the previous studies that the classical plate theory gives acceptable results only for thin plates and it is not suitable especially for advanced composite material plates and thick plates. In order to overcome the shortcomings of the classical plate theory, similar to the Timoshenko beam theory, the first order shear deformation theory is proposed by Mindlin [5] and Reissner [6]. A classical plate theory is the three-degrees of freedom theory, whereas the first order shear deformation plate theory is the five degrees of freedom plate model. In the application of this theory a shear correction coefficient is used in order to satisfy the plate boundary conditions at the top and bottom surfaces of the plate. According to the 3-D elasticity theory, the transverse shear stress distribution in the thickness direction of plate is approximately parabolic. Different shear deformation theories have been proposed during the last 6–7 decades, including polynomial [1, 6, 7], trigonometric [2, 4, 8], exponential [3, 9, 10]. A general shear deformable plate theory has been proposed and used by Timarci and Soldatos [11] for dynamic analysis of laminated shells and Aydogdu and Timarci [12], Timarci and Aydogdu [13], Aydogdu [14] for statics and dynamics of composite plates.

Later, some new functions were proposed by Reddy [1], Touratier [8], Soldatos [2], Karama *et al.* [3]. Different shear deformation theories were compared for dynamic and static analysis of laminated composites [14].

In addition to ESLT, the layer-wise theories and individual layer theories have been proposed to predict composite behaviour on the ply level by Wu and Chen [15] and Cho *et al.* [16]. These theories are often computationally more expensive to obtain accurate results. Recently, Abrate and Di Sciuva [17] have reviewed the single layer shear deformation theories. The following conditions are satisfied by the shear deformation theories considered in the literature:

– transverse shear stresses are zero at the top and bottom surfaces and nonzero elsewhere,

– approximately parabolic transverse shear stress distribution.
In the previous studies generally, the same shape function has been used in the in-plane directions. The shape function may change depending on material properties, boundary conditions and the aspect ratio of the plates.

The main novelty of the present study is to investigate the possibility of the different shear deformation theories in the different in-plane directions. The motivation of the study comes from the different material properties in different vertical planes in a laminated composite structure. Therefore, identical and different shear deformation theories will be used in the different in-plane direction in order to obtain static and dynamic response of composite plates.

In the present study, following additional assumptions are considered.

– 2-D results should be less than 3-D results,

– depending on the lamination configuration possibility of using different shape functions in different in-plane directions.

Validity of superposed shape functions was checked by comparing obtained results with existing 3-D and various 2-D results for bending, stress, vibration and buckling of symmetric cross-ply composite plates. Combinations of four generally used shear deformation theories have been constructed. Parabolic, hyperbolic, exponential and inverse trigonometric theories were used. These theories were denoted as R, S, E and T, respectively.

2. Laminated composite plates

Consider a rectangular plate with dimensions (a, b, h) where a and b are the in-plane dimensions, and h is the thickness of the plate. The plate is assumed to be constructed of linearly elastic orthotropic layers.

2.1. Displacement field

In this work, a displacement based equivalent single layer five degrees of freedom shear deformation theory is used for laminated composite plates. The following displacement field is generally used for a shear deformation plate theory (a theory with the following kinematic assumption) [7, 9, 11–14]:

$$
\begin{aligned}
U(x, y, z; t) &= u(x, y; t) - z w_{,x} + f(z) u_1(x, y; t), \\
V(x, y, z; t) &= v(x, y; t) - z w_{,y} + g(z) v_1(x, y; t), \\
W(x, y, z; t) &= w(x, y; t),
\end{aligned}
$$

(2.1)

where U, V and W are the displacement components along the x, y and z directions respectively, and u, v and w are the displacement of a point at the mid-plane along the x, y and z directions, respectively. Here u_1 and v_1 are the shear deformations measured at the mid-plane of the plate. $f(z)$ and $g(z)$ represent shape functions determining the distribution of the transverse shear strains and stresses along the thickness of the plate. A detailed check of the previously published papers showed that, generally the shear strain shape functions were chosen as the same functions in x and y directions (i.e. $f = g$). Considering different material properties along the thickness direction of a laminated composite plate in the x–z and y–z planes (Fig. 1), choosing different shape functions in the x and y directions may increase the accuracy of the obtained results.

In the present study, different functions were chosen from the literature as a shape function in order to represent the transverse shear stress distributions. Most common used four shape functions are listed in Table 1.

Top-bottom stiff in-x direction   *mid-stiff in y-direction*
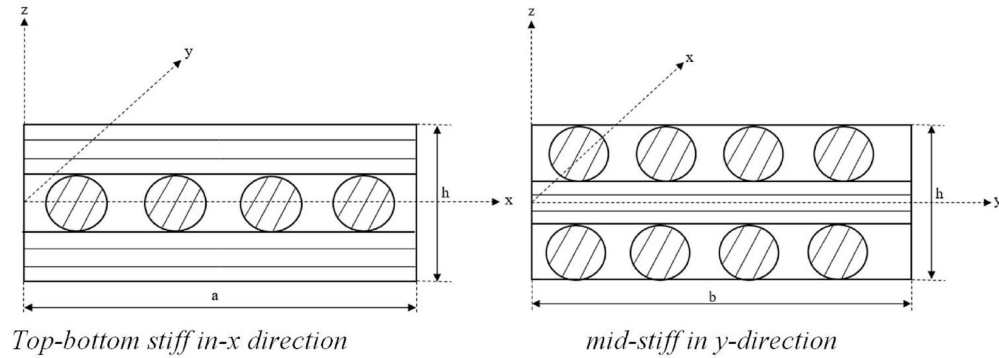
Fig. 1. 1-Composite plate cross-sections in x-z and y-z planes.

Table 1. Different transverse shear deformation functions.

Model	Function
Reddy (1984) [1], Reddy Model	$f(z) = z\left(1 - \dfrac{4z^2}{3h^2}\right)$
Soldatos (1992) [2]	$f(z) = h\sinh\left(\dfrac{z}{h}\right) - z\cosh\left(\dfrac{1}{2}\right)$
Karama *et al.* (1998) [3], KAM Model	$f(z) = ze^{-2(z/h)^2}$
Thai *et al.* (2014) [4]	$f(z) = ha\tan\left(\dfrac{2z}{h}\right) - z$

These shape functions satisfy the zero stress boundary conditions at the top and bottom surfaces of the plate and there is no need to use a shear correction factor which is used in the first order shear deformation theories. Combinations of these four functions were used in Eq. (2.1) as a shape function in this study.

2.2. Strain displacement relations

The displacement model given in Eq. (2.1) yields the following kinematic relations:

$$(2.2) \quad \begin{Bmatrix} \varepsilon_x \\ \varepsilon_y \\ \gamma_{xy} \\ \gamma_{xz} \\ \gamma_{yz} \end{Bmatrix} = \begin{Bmatrix} u_{,x} \\ v_{,y} \\ u_{,y} + v_{,x} \\ 0 \\ 0 \end{Bmatrix} - z \begin{Bmatrix} w_{,xx} \\ w_{,yy} \\ 2w_{,xy} \\ 0 \\ 0 \end{Bmatrix} + \begin{Bmatrix} f(z)u_{1,x} \\ g(z)v_{1,y} \\ (f(z)u_{1,y} + g(z)v_{1,x}) \\ f'u_1 \\ g'v_1 \end{Bmatrix}$$

where a prime denotes the derivative with respect to z and "$_{,x}$" and "$_{,y}$" represent partial derivatives with respect to x and y, respectively. The first two parenthesis

on the right-hand side of Eq. (2.2) belong to the classical plate theory, and the third one is due to the contribution of the transverse shear deformation.

2.3. Hooke's law

Stress strain relations in the kth layer of the composite plate are given by Hooke's Law as follows. It should be noted that $\sigma_z = 0$ is assumed in the present study:

$$(2.3) \quad \begin{bmatrix} \sigma_x^{(k)} \\ \sigma_y^{(k)} \\ \tau_{yz}^{(k)} \\ \tau_{xz}^{(k)} \\ \tau_{xy}^{(k)} \end{bmatrix} = \begin{bmatrix} \bar{Q}_{11}^{(k)} & \bar{Q}_{12}^{(k)} & 0 & 0 & 0 \\ \bar{Q}_{12}^{(k)} & \bar{Q}_{22}^{(k)} & 0 & 0 & 0 \\ 0 & 0 & \bar{Q}_{44}^{(k)} & 0 & 0 \\ 0 & 0 & 0 & \bar{Q}_{55}^{(k)} & 0 \\ 0 & 0 & 0 & 0 & \bar{Q}_{66}^{(k)} \end{bmatrix} \begin{bmatrix} \varepsilon_x \\ \varepsilon_y \\ \gamma_{yz} \\ \gamma_{xz} \\ \gamma_{xy} \end{bmatrix}$$

where $\bar{Q}_{ij}^{(k)}$ are the well-known reduced stiffnesses and k is the layer number [18]. Where the reduced stiffnesses are

$$(2.4) \quad \begin{bmatrix} \bar{Q}_{11} \\ \bar{Q}_{12} \\ \bar{Q}_{22} \\ \bar{Q}_{16} \\ \bar{Q}_{26} \\ \bar{Q}_{66} \\ \bar{Q}_{44} \\ \bar{Q}_{45} \\ \bar{Q}_{55} \end{bmatrix} = \begin{bmatrix} c^4 & 2s^2c^2 & s^4 & 4c^2s^2 & 0 & 0 \\ c^2s^2 & c^4 + s^4 & c^2s^2 & -4c^2s^2 & 0 & 0 \\ s^4 & 2c^2s^2 & c^4 & 4c^2s^2 & 0 & 0 \\ c^3s & cs^3 - c^3s & -cs^3 & -2cs(c^2 - s^2) & 0 & 0 \\ cs^3 & c^3s - cs^3 & -c^3s & 2cs(c^2 - s^2) & 0 & 0 \\ c^2s^2 & -2c^2s^2 & c^2s^2 & (c^2 - s^2)^2 & 0 & 0 \\ 0 & 0 & 0 & 0 & c^2 & s^2 \\ 0 & 0 & 0 & 0 & -cs & -cs \\ 0 & 0 & 0 & 0 & s^2 & c^2 \end{bmatrix} \begin{bmatrix} Q_{11} \\ Q_{12} \\ Q_{22} \\ Q_{66} \\ Q_{44} \\ Q_{55}. \end{bmatrix}.$$

Q_{ij}'s is defined as:

$$(2.5) \quad \begin{aligned} Q_{11} &= \frac{E_1}{1 - \nu_{12}\nu_{21}}, \\ Q_{12} &= Q_{21} = \frac{\nu_{12}E_2}{1 - \nu_{12}\nu_{21}}, \\ Q_{22} &= \frac{E_2}{1 - \nu_{12}\nu_{21}}, \\ Q_{44} &= G_{23}, \\ Q_{55} &= G_{13}Q_{12}, \end{aligned}$$

where E_i, G_{ij} and v_{ij} $(i, j = 1, 2)$ are the elasticity modulus, the shear modulus and the Poisson ratios.

2.4. Hamilton's principle

The strain energy, kinetic energy and work done by external in-plane loads can be written in the following form [19–20]:

$$(2.6) \qquad U_G = \frac{1}{2}\int_V (\sigma_x\varepsilon_x + \sigma_y\varepsilon_y + \tau_{xy}\gamma_{xy} + \tau_{xz}\gamma_{xz} + \tau_{yz}\gamma_{yz})dV,$$

$$(2.7) \qquad T = \frac{1}{2}\int_V \rho(U_{,t}^2 + V_{,t}^2 + W_{,t}^2)dV,$$

$$(2.8) \qquad V_L = \frac{1}{2}\int_A (N_x w_{,x}^2 + N_y w_{,y}^2 + 2N_{xy}w_{,x}w_{,y})dA,$$

where ρ is the density of the plate, V and A are the volume and the area of composite plate, respectively. ",$_t$" is the partial derivative with respect to time. Governing equations for bending, buckling and vibration can be found by applying Hamilton principles as follows [19]:

$$(2.9) \qquad \int_{t_0}^{t} (\delta U_G + \delta V_L - \delta T)dt = 0.$$

Here δ is the variational symbol. After inserting Eq. (2.6) to Eq. (2.8) into Eq. (2.9), the force and moment resultants are determined as:

$$(2.10) \qquad \begin{bmatrix} N_x^c \\ N_y^c \\ N_{xy}^c \\ M_x^c \\ M_y^c \\ M_{xy}^c \\ M_x^a \\ M_y^a \\ M_{xy}^a \\ M_{yx}^a \end{bmatrix} = \int_{-h/2}^{h/2} \begin{bmatrix} \sigma_x \\ \sigma_y \\ \tau_{xy} \\ z\sigma_x \\ z\sigma_y \\ z\tau_{xy} \\ f(z)\sigma_x \\ g(z)\sigma_y \\ f(z)\tau_{xy} \\ f(z)\tau_{xy} \end{bmatrix} dz,$$

$$(2.11) \qquad \begin{bmatrix} Q_x^a \\ Q_y^a \end{bmatrix} = \int_{-h/2}^{h/2} \begin{bmatrix} f'(z)\tau_{xz} \\ g'(z)\tau_{yz} \end{bmatrix} dz.$$

where N and M are the force and moment resultants, respectively. Q's are the shear force resultants, c and a denote the classical and additional (shear components) components respectively. A prime denotes derivative with respect to 'z' variable. By using Eqs. (2.3), (2.10) and (2.11) the following constitutive equations are obtained:

$$(2.12) \quad \begin{bmatrix} N_x^c \\ N_y^c \\ N_{xy}^c \\ M_x^c \\ M_y^c \\ M_{xy}^c \\ M_x^a \\ M_y^a \\ M_{xy}^a \\ M_{yx}^a \end{bmatrix} = \begin{bmatrix} A_{11} & A_{12} & A_{16} & B_{11} & B_{12} & B_{16} & E_{11} & \bar{E}_{12} & E_{16} & \bar{E}_{16} \\ A_{12} & A_{22} & A_{26} & B_{12} & B_{22} & B_{26} & E_{12} & \bar{E}_{22} & E_{16} & \bar{E}_{16} \\ A_{16} & A_{26} & A_{66} & B_{11} & B_{26} & B_{66} & E_{16} & \bar{E}_{26} & E_{66} & \bar{E}_{66} \\ B_{11} & B_{12} & B_{16} & D_{11} & D_{12} & D_{16} & F_{11} & \bar{F}_{12} & F_{16} & \bar{F}_{16} \\ B_{12} & B_{22} & B_{26} & D_{12} & D_{22} & D_{26} & F_{12} & \bar{F}_{22} & F_{26} & \bar{F}_{26} \\ B_{16} & B_{26} & B_{66} & D_{11} & D_{26} & D_{66} & F_{16} & \bar{F}_{26} & F_{66} & \bar{F}_{66} \\ E_{11} & E_{12} & E_{16} & F_{11} & F_{12} & F_{16} & H_{11} & \bar{H}_{12} & H_{16} & \bar{H}_{16} \\ E_{12} & E_{22} & E_{16} & F_{12} & F_{22} & F_{16} & H_{12} & \bar{H}_{22} & H_{26} & \bar{H}_{26} \\ E_{16} & E_{26} & E_{66} & F_{16} & F_{26} & F_{66} & H_{16} & \bar{H}_{26} & H_{66} & \bar{H}_{66} \\ E_{16} & E_{26} & E_{66} & F_{16} & F_{26} & F_{66} & H_{16} & \bar{H}_{26} & H_{66} & \bar{H}_{66} \end{bmatrix} \begin{bmatrix} u_{,x} \\ v_{,y} \\ u_{,y} + v_{,x} \\ -w_{,xx} \\ -w_{,yy} \\ -2w_{,xy} \\ u_{1,x} \\ v_{1,y} \\ u_{1,y} \\ v_{1,x} \end{bmatrix},$$

$$(2.13) \quad \begin{bmatrix} Q_y^a \\ Q_x^a \end{bmatrix} = \begin{bmatrix} A_{44} & 0 \\ 0 & A_{55} \end{bmatrix} \begin{bmatrix} v_1 \\ u_1 \end{bmatrix}.$$

The extensional (A_{ij}), coupling (B_{ij}), bending (D_{ij}) and transverse shear (F_{ij}, H_{ij}, E_{ij}) rigidities are defined as follows:

$$(2.14) \quad \begin{aligned}
A_{ij} &= \int_{-h/2}^{h/2} Q_{ij}^{(k)} dz, \quad A_{pq} = \int_{-h/2}^{h/2} Q_{pq}^{(k)} (f')^2 dz, \quad B_{ij} = \int_{-h/2}^{h/2} Q_{ij}^{(k)} z dz, \\
E_{ij} &= \int_{-h/2}^{h/2} Q_{ij}^{(k)} f(z) dz, \quad D_{ij} = \int_{-h/2}^{h/2} Q_{ij}^{(k)} z^2 dz, \quad F_{ij} = \int_{-h/2}^{h/2} Q_{ij}^{(k)} f(z) z dz, \\
H_{ij} &= \int_{-h/2}^{h/2} Q_{ij}^{(k)} (f)^2 dz, \quad \bar{E}_{ij} = \int_{-h/2}^{h/2} Q_{ij}^{(k)} g(z) dz, \quad \bar{F}_{ij} = \int_{-h/2}^{h/2} Q_{ij}^{(k)} g(z) z dz, \\
\bar{H}_{ij} &= \int_{-h/2}^{h/2} Q_{ij}^{(k)} (g)^2 dz, \qquad i,j,l,m = 1,2,6, \ p,q = 4,5, ( )' = d( )/dz.
\end{aligned}$$

2.5. Plate equations

Application of Hamilton's principle leads to following governing equations:

$$(2.15) \quad \begin{aligned}
& N_{x,x}^c + N_{xy,y}^c = (\rho_0 u - \rho_1 w_{,x} + \bar{\rho}_0^1 u_1)_{,tt}, \\
& N_{y,y}^c + N_{xy,x}^c = (\rho_0 v - \rho_1 w_{,y} + \bar{\rho}_0^1 v_1)_{,tt}, \\
& M_{x,xx}^c + M_{y,yy}^c + 2M_{xy,xy}^c + q + N_x^e w_{,xx} + N_y^e w_{,yy} + N_{xy}^e w_{,xy} \\
& \qquad = [\rho_0 w - \rho_1 v_{,y} - \rho_2(w_{,yy} + w) + \bar{\rho}_1^1 u_{1,x} + \bar{\rho}_1^1 v_{1,y} + \rho_1 u_{,x}]_{,tt}, \\
& M_{x,x}^a + M_{xy,y}^a - Q_x^a = (\bar{\rho}_0^1 u - \bar{\rho}_1^1 w_{,x} + \bar{\rho}_0^2 u_1)_{,tt}, \\
& M_{y,y}^a + M_{yx,y}^a - Q_y^a = (\bar{\rho}_0^1 v - \bar{\rho}_1^1 w_{,y} + \bar{\rho}_0^2 v_1)_{,tt}.
\end{aligned}$$

Here q is a transverse load, N_x^e, N_y^e and N_{xy}^e are the constant in-plane edge loads. The inertias ρ_i and $\bar{\rho}_i^m$ are defined by

(2.16)
$$\rho_i = \int_{-h/2}^{h/2} \rho z^i dz, \quad (i = 0, 1, 2),$$

$$\bar{\rho}_i^m = \int_{-h/2}^{h/2} \rho z^i f^m dz, \quad (i = 0, 1; \ m = 1, 2)$$

where ρ is the mass of the composite plate per unit volume.

2.6. Boundary conditions

The following edge boundary conditions should be satisfied,

(2.17)

At $x = 0$, a	at $y = 0$, b
either u or N_x^c prescribed,	either v or N_y^c prescribed,
either v or N_{xy}^c prescribed,	either u or N_{xy}^c prescribed,
either w or $M_{x,x}^c + 2M_{xy,y}^c$ prescribed,	either w or $M_{y,y}^c + 2M_{yx,x}^c$ prescribed,
either $w_{,x}$ or M_x^c prescribed,	either $w_{,y}$ or M_y^c prescribed,
either u_1 or M_x^a prescribed,	either u_1 or M_{yx}^a prescribed,
either v_1 or M_{xy}^a prescribed,	either v_1 or M_y^c prescribed.

It should be noted that for the present bifurcation buckling problem the boundary conditions are $N_x^c = 0$, $N_y^c = 0$ and $N_{xy}^c = 0$.

3. Exact solutions for symmetric cross-ply plates

In this study, statics and dynamics of simply supported, symmetric cross-ply rectangular composite plates were investigated as generally considered in the open literature. The Navier solution method was used in the solution of the problems. For symmetric cross-ply plates, the following plate stiffness components (Eq. 2.14) are identically zero.

(3.1)
$$A_{16} = A_{26} = D_{16} = D_{26} = F_{16} = F_{26} = H_{16} = H_{26} = 0,$$
$$B_{ij} = 0 \text{ and } E_{ij} = 0, \quad ij = 1, 2.$$

Thus, the coupling between stretching and bending is zero. The following simply supported boundary conditions are assumed.

(3.2)
$$w = M_x^c = M_x^a = v_1 = 0 \quad \text{at } x = 0 \text{ and } a,$$
$$w = M_y^c = M_y^a = v_1 = 0 \quad \text{at } y = 0 \text{ and } b.$$

According to the Navier method following choice of the displacement components satisfy the boundary conditions and the governing equations

$$w = \sum_{m,n=1}^{\infty} W_{mn} \sin(\alpha x) \sin(\beta y) \sin(\omega t),$$

(3.3)
$$(au_1) = \sum_{m,n=1}^{\infty} X_{mn} \cos(\alpha x) \sin(\beta y) \sin(\omega t),$$

$$(bv_1) = \sum_{m,n=1}^{\infty} Y_{mn} \sin(\alpha x) \cos(\beta y) \sin(\omega t),$$

where $\alpha = m\pi/a$, $\beta = n\pi/b$ and m and n are the half-wave numbers along the x and y directions, respectively. For the static problems $\sin \omega t = 1$ was used.

3.1. Bending analysis

The transverse load acting on the composite plate upper surface can be written in the following double Fourier series form

(3.4)
$$q = \sum_{m,n=1}^{\infty} Q_{mn} \sin(\alpha x) \sin(\beta y),$$

where Q_{mn} is the amplitude of the force. Substituting Eqs. (3.3)–(3.4) into the Eq. (2.15) and after some algebra, following equations are obtained for any fixed values of m and n

(3.5)
$$\begin{bmatrix} L_{11} & L_{12} & L_{13} \\ & L_{22} & L_{23} \\ sym & & L_{33} \end{bmatrix} \begin{bmatrix} W_{mn} \\ X_{mn} \\ Y_{mn} \end{bmatrix} = \begin{bmatrix} Q_{mn} \\ 0 \\ 0 \end{bmatrix}.$$

The elements L_{ij} of the coefficient matrix [L] are

(3.6)
$$\begin{aligned}
L_{11} &= D_{11}\alpha^4 + 2\lambda^2(D_{12} + 2D_{66})\alpha^2\beta^2 + \lambda^4 D_{22}\beta^4, \\
L_{12} &= F_{11}\alpha^3 + \lambda^2(F_{12} + 2F_{66})\alpha\beta^2, \\
L_{13} &= \lambda(F_{12} + 2F_{66})\alpha^2\beta + \lambda^3 F_{22}\beta^3, \\
L_{21} &= L_{12}, \\
L_{22} &= H_{11}\alpha^2 + \lambda^2 H_{66}\beta^2 - A_{55}, \\
L_{23} &= \lambda(H_{12} + H_{66})\alpha\beta, \\
L_{31} &= L_{13}, \qquad L_{32} = L_{23}, \\
L_{33} &= H_{66}\alpha^2 + \lambda^2 H_{22}\beta^2 - A_{44},
\end{aligned}$$

where $\lambda = a/b$. Solution of the Eq. (3.4) gives amplitudes of displacements. Using Eq. (2.3) and Eq. (2.9) all stress components can be obtained. For a sinusoidal distributed load the following relation can be written using Eq. (3.4)

$$(3.7) \qquad q(xy) = q_0 \sin \frac{m\pi x}{a} \sin \frac{n\pi y}{b},$$

where $m = n = 1$, and $q_0 = Q_{11}$.

In the present study, all of the stress components were computed from constitutive equations. Transverse normal stress was not given in this study.

3.2. Buckling and vibration problem

The vibration frequency and critical buckling load of a uniformly in-plane loaded cross-ply composite plate with all edges simply supported can be determined by using Eq. (2.15) and Eq. (3.3). For this case $q = 0$ and $\rho = 0$ were used in Eq. (2.15). Substituting Eq. (3.3) into Eq. (2.15) and collecting the like coefficients leads to the following eigenvalue equation for any fixed values of m and n:

$$(3.8) \qquad ([K] - \Omega^2 [M])\{\Delta\} = \{0\}, \qquad \{\Delta\}^T = \{W_{mn}, X_{mn}, Y_{mn}\}.$$

Here $[K]$ is the stiffness matrix and $[M]$ is the mass matrix in the case of vibration and geometric matrix due to the in-plane forces in the case of buckling, and the parameter Ω refers to the corresponding buckling or frequency parameter. It should be noted that the solution of Eq. (3.8) gives three roots for fixed m and n. The lowest of them is a critical buckling load parameter in the buckling problem and they are three distinct frequencies in the vibration problem. If required one can obtain corresponding mode shapes by inserting the eigenvalue Ω into Eq. (3.8).

4. Numerical results

In the present study, bending, buckling and vibration results were determined for symmetric cross-ply plates using superposed shape functions in a general shear deformation plate theory. The following material properties are used in the analysis:

Material 1 [1]: $E_1 = 174.6$ GPa, $E_2 = 7$ GPa, $G_{12} = G_{13} = 3.5$ GPa, $G_{23} = 1.4$ GPa, $\nu_{12} = \nu_{13} = 0.25$.

Material 2: $E_1/E_2 = $ open, $G_{12} = 0.6E_2$, $G_{23} = 0.5\ E_2$, $\nu_{12} = 0.25$.

It is assumed further that $G_{13} = G_{12}$, $\nu_{13} = \nu_{12}$ and $\rho = 1$.

4.1. Bending and stress analysis for laminated composite plates

In this section bending and stresses of a transversely loaded simply supported symmetric cross-ply plate were given. The non-dimensional deflections and stresses are defined as:

$$\bar{w} = \frac{w\left(\frac{a}{2}, \frac{a}{2}, 0\right) E_2 h^3}{q_0 a^4} \times 100, \quad \bar{\sigma}_x = \sigma_x \left(\frac{a}{2}, \frac{a}{2}, \frac{h}{2}\right) \frac{h^2}{q_0 a^2},$$

(4.1)
$$\bar{\sigma}_y = \sigma_y \left(\frac{a}{2}, \frac{a}{2}, \frac{h}{4}\right) \frac{h^2}{q_0 a^2}, \quad \bar{\tau}_{xy} = \tau_{xy} \left(0, 0, \frac{h}{2}\right) \frac{h^2}{q_o a^2},$$

$$\bar{\tau}_{yz} = \tau_{yz} \left(\frac{a}{2}, 0, 0\right) \frac{h}{q_0 a}, \quad \bar{\tau}_{xz} = \tau_{xz} \left(0, \frac{a}{2}, 0\right) \frac{h}{q_0 a}.$$

The combinations of the four shape functions listed in Table 1 lead to 16 possibilities which can be used as a shape function in the x and y directions. They are R-R, F-F, S-S, K-K, R-F, F-R, R-S, S-R, S-F, F-S, K-R, R-K, S-K, K-S, K-F and F-K. Here the first and second letters denote the shape function along the x and y directions.

Two example problems have been used in order to investigate the effect of using different shape functions in the in-plane directions. In the first case, the non-dimensional deflections and stresses under sinusoidal load obtained for four-layers cross-ply ($0°/90°/90°/0°$) laminates using the shape functions stated above for various values of thickness parameter a/h and compared with the previously published results [1, 21] in Tables 2–5. The second example problem is for three-layers cross ply ($0°/90°/0°$) laminates using various values of thickness parameter a/h which are compared with the previously published results [1, 22] in Tables 6–9.

It should be noted that approximate theories should predict stiffer mechanical behaviour when compared to the 3-D elasticity results. Therefore, the deflection and stress values predicted by shear deformation theories should be less than the 3-D results and vibration frequencies and buckling loads should be higher than the corresponding 3-D counterparts. This fact is generally used in the literature only for the classical plate theories but it has not been considered for shear deformation theories. After comparing the present, bending and stress results with the 3-D elasticity solutions, except R-R, S-S, R-S, S-R, R-K and S-K models all the other models give some of the static results higher than that of the 3-D elasticity results. This fact has been summarised in Table 10. If a theory predicts flexible properties with respect to 3-D elasticity it is denoted with a "+" sign in Table 10 for the corresponding stress components. So, the theories with at least one "+" sign are not used in the remaining part of the study due to their flexible behaviour predictions compared to 3-D elasticity. It is observed that σ_{xz} stress is predicted less than 3-D elasticity by some of the theories for four layer cross-ply

Table 2. Comparison of non-dimensionalized deflections and stresses under sinusoidal transverse loads with 3-D results ($a/b = 1$, $(0°/90°/90°/0°)$, Material 1) (3-D: Pagano and Hatfield [21]).

a/h	theory	w	σ_{xx}	σ_{yy}	σ_{yz}	σ_{xz}	σ_{xy}
4	3-D	1.954	0.720	0.663	0.292	0.219	0.0467
	R-R	1.8946	0.6645	0.6315	0.2389	0.2064	0.04409
	F-F	1.9268	0.7148	0.6377	0.2624	0.2397	0.004680
	S-S	1.8930	0.6629	0.6313	0.2382	0.2055	0.04400
	K-K	1.9203	0.6997	0.6360	0.2531	0.2265	0.04598
	R-F	1.9031	0.6673	0.6291	0.2598	0.2074	0.04542
	F-R	1.9183	0.7118	0.6400	0.2412	0.2385	0.04546
	R-S	1.8943	0.6644	0.6317	0.2383	0.2064	0.04405
	S-R	1.8934	0.6630	0.6310	0.2387	0.2055	0.04438
	S-F	1.9018	0.6658	0.6287	0.2597	0.2066	0.04536
	F-S	1.9180	0.7116	0.6402	0.2406	0.2385	0.04542
	K-R	1.9147	0.6977	0.6387	0.2410	0.2258	0.04511
	R-K-	1.9002	0.6664	0.6289	0.2509	0.2070	0.04495
	S-K	1.8989	0.6649	0.6284	0.2508	0.2062	0.04490
	K-S	1.9144	0.6976	0.6389	0.2404	0.2257	0.04507
	K-F	1.9232	0.7007	0.6363	0.2621	0.2269	0.04645
	F-K	1.9238	0.7138	0.6375	0.2633	0.2393	0.04633

Table 3. Comparison of non-dimensionalized deflections and stresses under sinusoidal transverse loads with previously published results ($a/b = 1$, $(0°/90°/90°/0°)$, Material 1) (3-D: Pagano and Hatfield [21]).

a/h	theory	w	σ_{xx}	σ_{yy}	σ_{yz}	σ_{xz}	σ_{xy}
10	3-D	0.743	0.559	0.401	0.196	0.301	0.0275
	R-R	0.7156	0.5454	0.3884	0.1530	0.2640	0.02680
	F-F	0.7281	0.5554	0.3939	0.1704	0.3133	0.02738
	S-S	0.7151	0.5451	0.3882	0.1526	0.2627	0.02678
	K-K	0.7248	0.5523	0.3925	0.1634	0.2941	0.02721
	R-F	0.7162	0.5459	0.3875	0.1680	0.2642	0.02692
	F-R	0.7274	0.5449	0.3948	0.1551	0.3130	0.02726
	R-S	0.7155	0.5454	0.3885	0.1527	0.2640	0.02679
	S-R	0.7151	0.5451	0.3882	0.1530	0.2627	0.02678
	S-F	0.7157	0.5456	0.3872	0.1680	0.2629	0.02690
	F-S	0.7274	0.5548	0.3949	0.1547	0.3130	0.02725
	K-R	0.7244	0.5520	0.3932	0.1546	0.2939	0.02713
	R-K	0.7159	0.5457	0.3877	0.1617	0.2642	0.02688
	S-K	0.7155	0.5454	0.3875	0.1616	0.2628	0.02685
	K-S	0.7244	0.5519	0.3933	0.1542	0.2939	0.02713
	K-F	0.7251	0.5525	0.3923	0.1698	0.2942	0.02725
	F-K	0.7278	0.5552	0.3941	0.1639	0.3132	0.02733

Table 4. Comparison of non-dimensionalized deflections and stresses under sinusoidal transverse loads with previously published results ($a/b = 1$, ($0°/90°/90°/0°$), Material 1) (3-D: Pagano and Hatfield [21]).

a/h	theory	w	σ_{xx}	σ_{yy}	σ_{yz}	σ_{xz}	σ_{xy}
20	3-D	0.517	0.543	0.308	0.156	0.328	0.0230
	R-R	0.507	0.5391	0.3041	0.1234	0.2825	0.02284
	F-F	0.511	0.5417	0.3062	0.1366	0.3372	0.02300
	S-S	0.507	0.5391	0.3041	0.1231	0.2810	0.02284
	K-K	0.509	0.5409	0.3055	0.1311	0.3160	0.02296
	R-F	0.507	0.5392	0.3039	0.1358	0.2825	0.02286
	F-R	0.510	0.5416	0.3062	0.1242	0.3372	0.02298
	R-S	0.507	0.5391	0.3041	0.1231	0.2825	0.02284
	S-R	0.507	0.5391	0.3040	0.1234	0.2810	0.02284
	S-F	0.507	0.5392	0.3038	0.1358	0.2810	0.02286
	F-S	0.511	0.542	0.306	0.124	0.337	0.02298
	K-R	0.510	0.541	0.306	0.124	0.316	0.02294
	R-K	0.507	0.539	0.304	0.131	0.283	0.02286
	S-K	0.507	0.539	0.304	0.131	0.281	0.02285
	K-S	0.510	0541	0.306	0.124	0.316	0.02294
	K-F	0.510	0.541	0.306	0.136	0.316	0.02296
	F-K	0.510	0.542	0.306	0.131	0.337	0.02299

Table 5. Comparison of non-dimensionalized deflections and stresses under sinusoidal transverse loads with previously published results ($a/b = 1$, ($0°/90°/90°/0°$), Material 1) (3-D: Pagano and Hatfield [21]).

a/h	theory	w	σ_{xx}	σ_{yy}	σ_{yz}	σ_{xz}	σ_{xy}
100	3-D	0.4385	0.539	0.276	0.141	0.337	0.0216
	R-R	0.435	0.539	0.271	0.112	0.2897	0.0214
	F-F	0.4353	0.5387	0.2708	0.1230	0.3467	0.02139
	S-S	0.4352	0.5386	0.2707	0.112	0.2881	0.0214
	K-K	0.4353	0.5386	0.2708	0.1182	0.3246	0.02139
	R-F	0.4352	0.5389	0.2707	0.1229	0.2897	0.02139
	F-R	0.4353	0.5387	0.2708	0.1118	0.3467	0.02139
	R-S	0.4352	0.5386	0.2708	0.112	0.2897	0.0214
	S-R	0.4352	0.5386	0.2707	0.112	0.2882	0.0214
	S-F	0.4352	0.5386	0.2707	0.1230	0.2881	0.02139
	F-S	0.435	0.539	0.271	0.112	0.347	0.0214
	K-R	0.435	0.539	0.271	0.112	0.325	0.0214
	R-K	0.435	0.539	0.271	0.118	0.290	0.0214
	S-K	0.435	0.539	0.271	0.118	0.288	0.0214
	K-S	0.435	0.539	0.271	0.112	0.325	0.0214
	K-F	0.435	0.539	0.271	0.123	0.325	0.0214
	F-K	0.435	0.539	0.271	0.118	0.347	0.0214

Table 6. Comparison of non-dimensionalized deflections and stresses under sinusoidal transverse loads with previously published results ($a/b = 1$, ($0°/90°/0°$), Material 1) (3-D: Pagano [22]).

a/h	theory	w	σ_{xx}	σ_{yy}	σ_{yz}	σ_{xz}	σ_{xy}
4	3-D	2.006	0.755	0.556	0.217	0.282	0.0505
	R-R	1.9226	0.7337	0.502	0.1832	0.2024	0.04976
	F-F	1.9524	0.7940	0.5016	0.1974	0.2332	0.05261
	S-S	1.9213	0.7318	0.5019	0.1827	0.2016	0.04967
	K-K	1.9441	0.7750	0.5021	0.1918	0.2205	0.05167
	R-F	1.9191	0.7321	0.4927	0.1947	0.2021	0.05071
	F-R	1.9562	0.7957	0.5110	0.1857	0.2335	0.05165
	R-S	1.9227	0.7337	0.5023	0.1828	0.2024	0.04973
	S-R	1.9212	0.7317	0.5016	0.1830	0.2016	0.04969
	S-F	1.9176	0.7302	0.4923	0.1946	0.2013	0.05064
	F-S	1.9563	0.7957	0.5113	0.1854	0.2335	0.05163
	K-R	1.9462	0.7759	0.5083	0.1850	0.2207	0.05106
	R-K	1.9206	0.7328	0.4959	0.1899	0.2022	0.05037
	S-K	1.9192	0.7309	0.4955	0.1898	0.2014	0.05030
	K-S	1.9462	0.7760	0.5086	0.1847	0.2207	0.05103
	K-F	1.9424	0.7743	0.4989	0.1966	0.2204	0.05202
	F-K	1.9541	0.7947	0.5048	0.1925	0.2333	0.05227

Table 7. Comparison of non-dimensionalized deflections and stresses under sinusoidal transverse loads with previously published results ($a/b = 1$, ($0°/90°/0°$), Material 1) (3-D: Pagano [22]).

a/h	theory	w	σ_{xx}	σ_{yy}	σ_{yz}	σ_{xz}	σ_{xy}
10	3-D	0.7405	0.590	0.288	0.123	0.357	0.0289
	R-R	0.7133	0.5681	0.2687	0.1033	0.2446	0.02771
	F-F	0.7297	0.5811	0.2740	0.1119	0.2924	0.0284
	S-S	0.7127	0.5677	0.2685	0.1031	0.2434	0.02768
	K-K	0.7239	0.5768	0.2721	0.1085	0.2727	0.02819
	R-F	0.7131	0.5680	0.2679	0.1099	0.2446	0.02780
	F-R	0.7298	0.5812	0.2748	0.1052	0.2924	0.02836
	R-S	0.7133	0.5681	0.2687	0.1032	0.2446	0.02770
	S-R	0.7127	0.5677	0.2685	0.1033	0.2434	0.02469
	S-F	0.7126	0.5676	0.2677	0.1099	0.2434	0.02778
	F-S	0.7298	0.5812	0.2749	0.1050	0.2924	0.02835
	K-R	0.7240	0.5769	0.2727	0.1046	0.2727	0.02813
	R-K	0.7132	0.5680	0.2681	0.1072	0.2446	0.02776
	S-K	0.7126	0.5676	0.2679	0.1071	0.2434	0.02774
	K-S	0.7240	0.5769	0.2727	0.1044	0.2727	0.02813
	K-F	0.7238	0.5767	0.2719	0.1112	0.2727	0.02822
	F-K	0.7297	0.5812	0.2743	0.1091	0.2924	0.02841

Table 8. Comparison of non-dimensionalized deflections and stresses under sinusoidal transverse loads with previously published results ($a/b = 1$, ($0°/90°/0°$), Material 1) (3-D: Pagano [22]).

a/h	theory	w	σ_{xx}	σ_{yy}	σ_{yz}	σ_{xz}	σ_{xy}
20	3-D	-	0.552	0.210	0.094	0.385	0.0234
	R-R	0.5049	0.5458	0.2041	0.08262	0.2548	0.0230
	F-F	0.5097	0.5492	0.2059	0.08839	0.3068	0.02323
	S-S	0.5048	0.5457	0.2041	0.08246	0.2535	0.02302
	K-K	0.508	0.5481	0.2053	0.08602	0.2854	0.02316
	R-F	0.5049	0.5458	0.2040	0.08777	0.2548	0.02305
	F-R	0.5098	0.5492	0.2060	0.08320	0.3068	0.02322
	R-S	0.5049	0.5458	0.2041	0.08247	0.2548	0.02303
	S-R	0.5048	0.5457	0.2041	0.08260	0.2535	0.02302
	S-F	0.5047	0.5457	0.2039	0.08775	0.2535	0.02304
	F-S	0.5098	0.5492	0.2060	0.08306	0.3068	0.02322
	K-R	0.508	0.5481	0.2054	0.0829	0.2854	0.02315
	R-K	0.5049	0.5458	0.2040	0.08563	0.2548	0.0230
	S-K	0.5047	0.5457	0.2040	0.08561	0.2535	0.02304
	K-S	0.5080	0.5481	0.2054	0.08285	0.2854	0.02315
	K-F	0.5080	0.5481	0.2052	0.08817	0.2854	0.02317
	F-K	0.5098	0.5492	0.2059	0.08624	0.3068	0.02323

Table 9. Comparison of non-dimensionalized deflections and stresses under sinusoidal transverse loads with previously published results ($a/b = 1$, ($0°/90°/0°$), Material 1) (3-D: Pagano [22]).

a/h	theory	w	σ_{xx}	σ_{yy}	σ_{yz}	σ_{xz}	σ_{xy}
100	3-D	-	0.539	0.181	0.083	0.395	0.0213
	R-R	0.435	0.539	0.181	0.075	0.259	0.0213
	F-F	0.435	0.5389	0.1806	0.079	0.3120	0.0214
	S-S	0.435	0.539	0.181	0.075	0.257	0.0213
	K-K	0.435	0.5389	0.1805	0.07780	0.2900	0.0213
	R-F	0.435	0.5388	0.18053	0.07970	0.2585	0.0213
	F-R	0.4352	0.5389	0.1806	0.07511	0.3120	0.0213
	R-S	0.435	0.539	0.181	0.075	0.259	0.0214
	S-R	0.435	0.539	0.181	0.075	0.257	0.0213
	S-F	0.435	0.5388	0.1805	0.07970	0.257	0.0213
	F-S	0.435	0.5389	0.1806	0.07498	0.312	0.0214
	K-R	0.435	0.5389	0.1805	0.07510	0.290	0.0213
	R-K	0.435	0.539	0.181	0.078	0.259	0.0213
	S-K	0.435	0.539	0.181	0.078	0.257	0.0213
	K-S	0.435	0.5389	0.1805	0.07497	0.290	0.0213
	K-F	0.435	0.5389	0.1805	0.07972	0.290	0.0213
	F-K	0.435	0.5389	0.1806	0.07781	0.312	0.0214

Table 10. Comparison of bending and stress values of higher order theories with 3-D elasticity results.

Theory	$0°/90°/90°/0°)$				$(0°/90°/0°)$			
	a/h				a/h			
	5	10	20	100	5	10	20	100
	σ_{xz}	σ_{xz}	σ_{xz}	σ_{xz}	σ_{xx},σ_{xy}			
R-R								
F-F	+	+	+	+	++			
S-S								
K-K	+				++			
R-F					+			
F-R	+	+	+	+	++			
R-S								
S-R								
S-F					+			
F-S	+	+	+	+	++			
K-R	+				++			
R-K								
S-K								
K-S	+				++			
K-F	+				++			
F-K	+	+	+	+	++			

composites whereas it is true for σ_{xx} and σ_{xy} stresses for three layer cross-ply composites.

The percentage difference given in Tables 2–9 is defined as follows:

$$(4.2) \qquad \%\text{Error} = \frac{\mu^e - \mu^p}{\mu^e} 100 \quad (\mu = \sigma_{ij}, \; w; \; i, j = x, y, z),$$

where μ^e corresponds to the exact value and μ^p represents results obtained in the present study by means of shear deformation theories.

Considering the results presented in Table 10, the percentage differences were computed only for R-R, S-S, R-S, S-R, R-K and S-K models. The shape functions and their derivatives used in this study were depicted in Fig. 2. According to figures a shape function has an inflection point at $z = 0$. Derivatives of shape functions have zero value at $z = -0.5$ and 0.5 nonzero elsewhere and they are maximum at $z = 0$.

The %Error of deflection and stresses have been presented in Figs. 3–8 as a function of a/h ratio for R-R, S-S, R-S, S-R, R-K and S-K models. According to these tables and figures (3–8), the percentage errors of w, σ_{xx}, σ_{yy} and σ_{xy}

Table 11. Comparison of non-dimensionalized vibration frequencies with previously published results ($a/b = 1$, $(0°/90°/90°/0°)$, Material 2) (A: Noor [23]; B: Phan and Reddy [24]).

		E1/E2				
a/h	Source	3	10	20	30	40
5	A	6.6815	8.2103	9.5603	10.272	10.752
	R-K	6.5986	8.5219	9.9447	10.676	11.051
	%Error	−1.24	3.79	4.02	3.93	2.78
	S-K	6.5984	8.5217	9.9432	10.674	11.048
	%Error	−1.24	3.79	4.00	3.91	2.75
	K-K	6.5625	8.2805	9.5420	10.292	10.810
	%Error	−1.78	0.85	0.19	0.19	0.53
	B	6.5597	8.2718	9.5263	10.272	10.787
	%Error	−1.82	0.74	0.35	0.00	0.32
	R-K	7.2576	9.9716	12.565	14.419	15.840
	S-K	7.2575	9.9715	12.564	14.417	15.839
10	K-K	7.2440	9.8446	12.227	13.879	15.127
	R-R	7.2433	9.8409	12.218	13.863	15.107
	R-K	7.4626	10.466	13.562	15.975	17.986
	S-K	7.4622	10.465	13.562	15.974	17.985
	K-K	7.4588	10.428	13.440	15.753	17.655
20	R-R	7.4586	10.426	13.437	15.747	17.646

Table 12. Comparison of non-dimensionalized buckling load parameters with previously published results ($a/b = 1$, $(0°/90°/90°/0°)$, Material 2) (A: Noor [25]; B: Phan and Reddy [24]).

		E1/E2				
a/h	Source	3	10	20	30	40
	K-K	4.5502	7.1711	9.4538	10.952	12.050
	R-R	4.5458	7.1554	9.4218	10.908	11.997
5	R-K	4.5474	7.1476	9.3967	10.8639	11.931
	S-K	4.5472	7.1473	9.3958	10.861	11.928
10	A	5.2944	9.7621	15.0191	19.3040	22.8807
	R-K	5.3937	9.9375	15.287	19.6530	23.305
	%Error	1.87	1.80	1.78	1.80	1.85
	S-K	5.3936	9.9374	15.287	19.651	23.303
	%Error	1.87	1.80	1.78	1.80	1.84
	K-K	5.3945	9.9480	15.322	19.717	23.402
	%Error	1.89	1.90	2.01	2.13	2.27
	B	5.1143	9.7740	15.298	19.957	23.340
	%Error	3.40	0.12	1.85	3.38	2.00
	R-R	5.3933	9.9405	15.298	19.674	23.340
	R-K	5.6591	11.0557	18.359	25.209	31.648
	S-K	5.6590	11.0556	18.359	25.209	31.648
20	K-K	5.6593	11.058	18.372	25.235	31.691
	R-R	5.6590	11.056	18.363	25.216	31.659

a)

b)
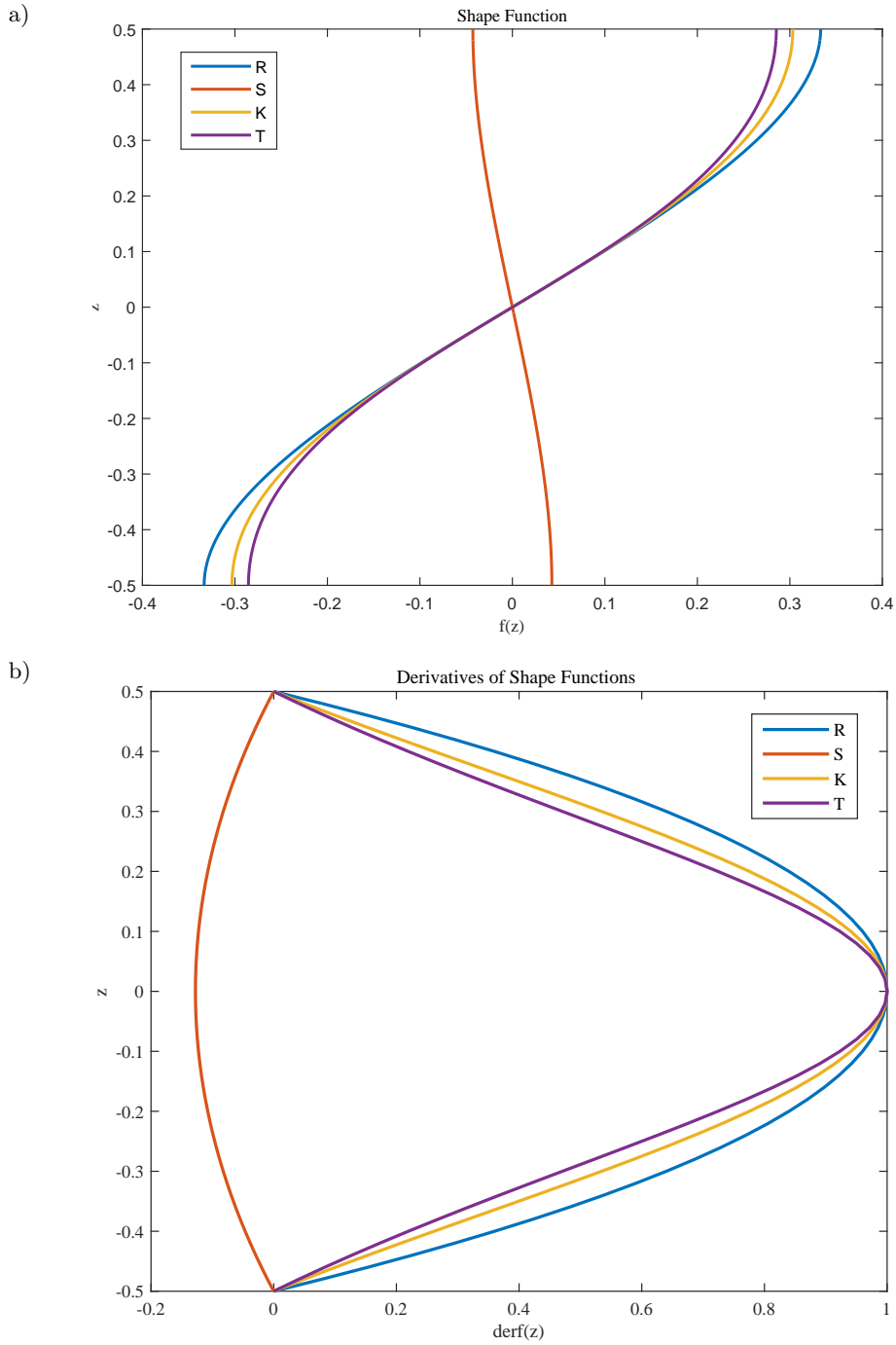
Fig. 2. Various shape functions used in the present study (R: Reddy [1], S: Soldatos [2], K: Karama *et al.* [3], T: Thai *et al* [4].)
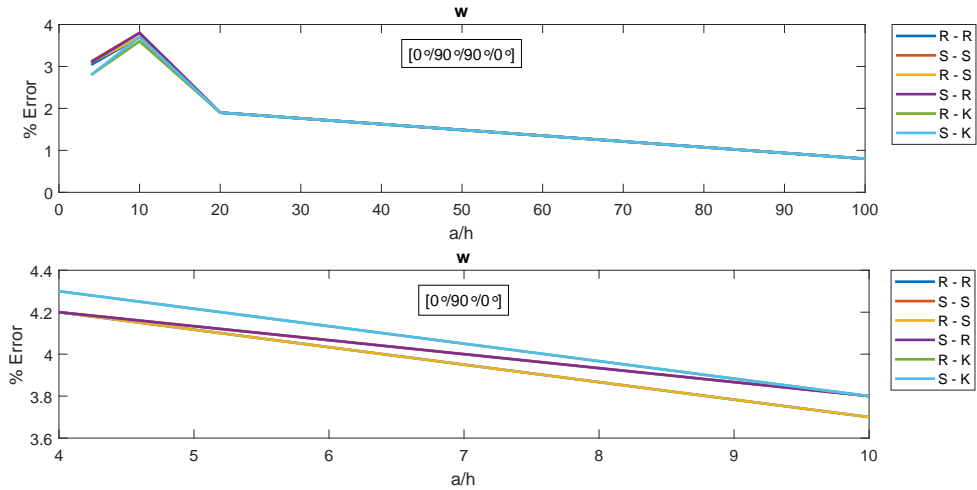
FIG. 3. Variation of percentage error of bending w with a/h ratio.
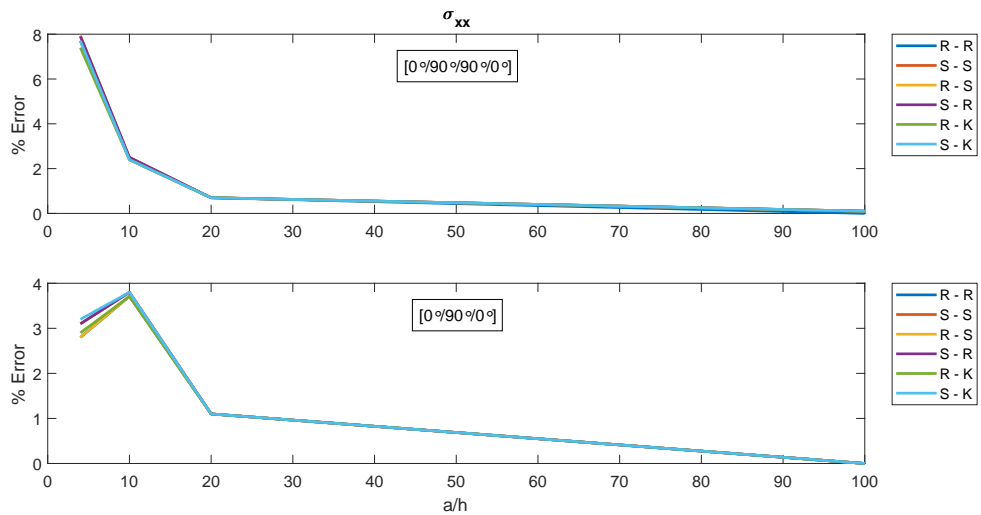
FIG. 4. Variation of percentage error of σ_{xx} with a/h ratio.

are less than %10. The %Error values decrease with increasing a/h ratio. This fact is especially true for the R-K and S-K models.

However, higher errors are observed for transverse shear stress components (σ_{xz} and σ_{yz}). The error of σ_{xz} for 4-layers cross-ply plates is between %13–15 whereas it is %33–35 for the 3-layers cross-ply composite plates when $a/h > 20$. There is no important effect of mixed shear deformation models on σ_{xz} com-
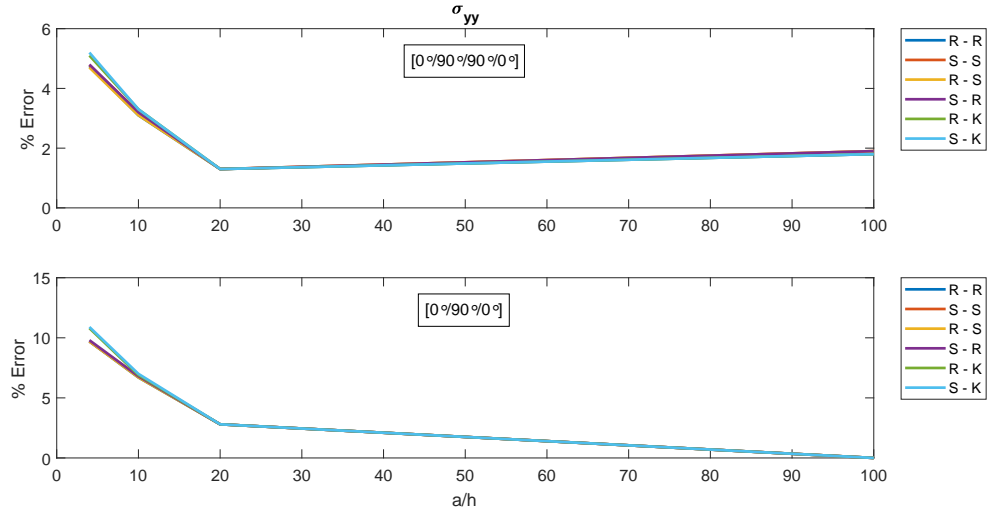
FIG. 5. Variation of percentage error of σ_{yy} with a/h ratio.
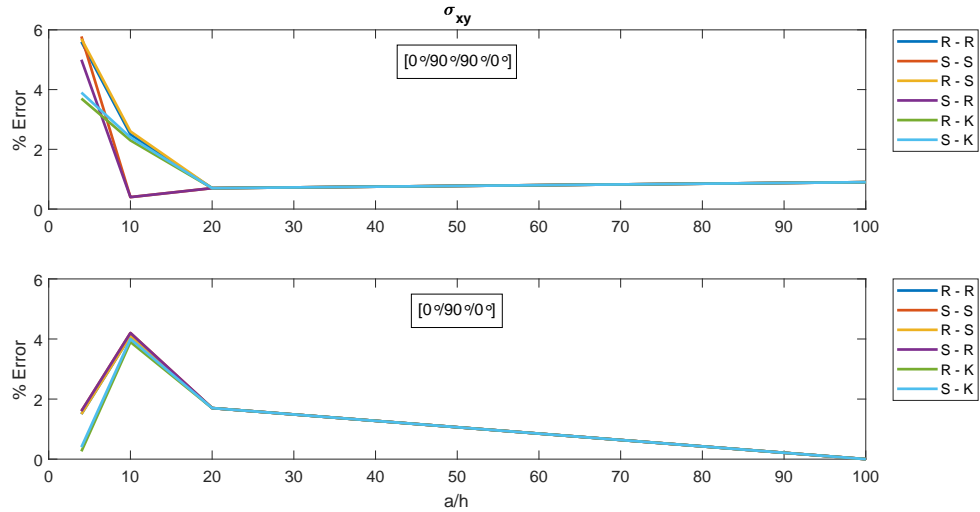
FIG. 6. Variation of percentage error of σ_{xy} with a/h ratio.

ponent of the stress. However, some reasonable improvements are observed for the σ_{yz} component of the shear stress components. R-K and S-K models have lower errors when compared to other models considered. The difference between other models and R-K and S-K increases with increasing a/h ratio. S-K model gives %8 lower errors when compared to other models (except R-K model) for
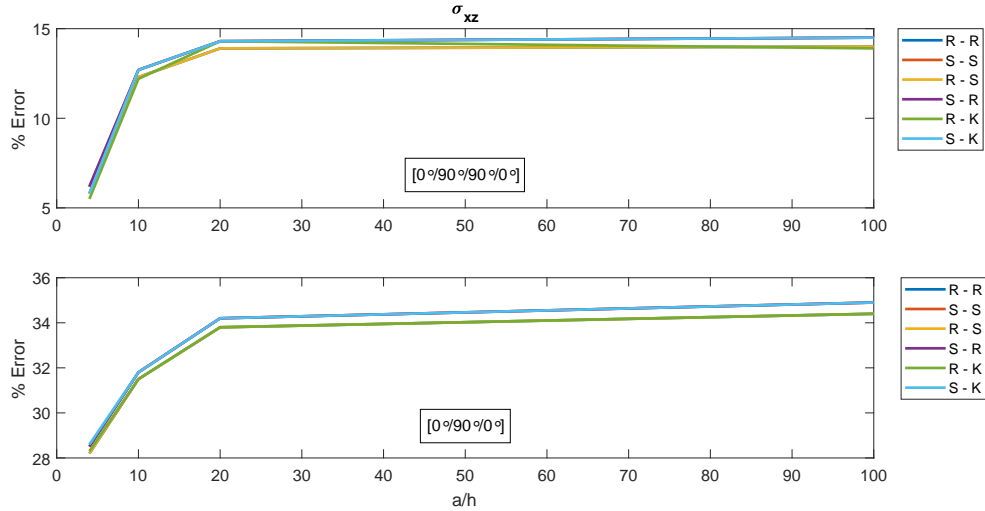
FIG. 7. Variation of percentage error of σ_{xz} with a/h ratio.
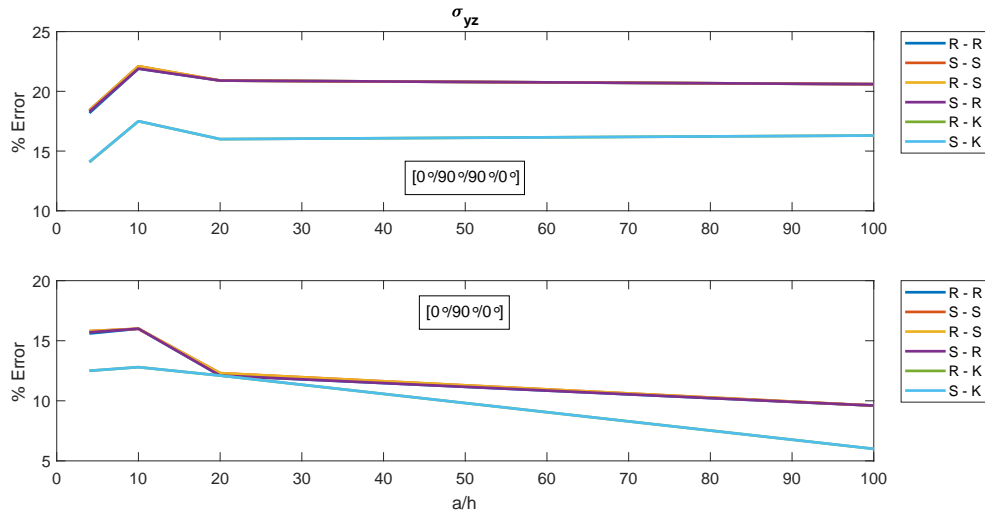
FIG. 8. Variation of percentage error of σ_{yz} with a/h ratio.

4-layers composite plates. Again S-K model predicts yz shear stress component with %3–4 smaller errors when compared to other models. It means that the K shape function is more appropriate for composite plates with low 90° layer thickness.

Satisfying continuity of transverse shear stress components may improve transverse shear stress terms, but this includes material properties. Continuity of transverse shear stresses is not considered in the present study.

4.2. Free flexural vibration analysis for laminated composite plates

The dimensionless natural frequency parameter is defined as $\Omega = (\omega a^2/h)(\rho/E_2)^{1/2}$. Comparison of the lowest natural frequencies of four layer symmetric cross-ply $(0°/90°/90°/0°)$ rectangular laminates with three-dimensional elasticity solutions of Noor [23] and parabolic shear deformation theory results of Phan and Reddy [24] for various values of the orthotrophy of individual layers E_1/E_2 and the various values of side to thickness ratio (a/h) is presented in Table 11 and the agreement is found to be good. It was obtained that the highest %Error between S-K, R-K and 3-D elasticity is less than %4.

4.3. Buckling analysis of laminated composite plates

The effects of transverse shear strain distribution on the buckling loads of plates subjected to in-plane uni-axial compressive loads were investigated. The dimensionless buckling load parameter is defined as $\Omega = N_x^e a^2/E_2 h^3$. The critical buckling load parameter of four layers symmetric cross-ply $(0°/90°/90°/0°)$ rectangular plates are determined and compared to 3-D linear elasticity solutions in Table 12 and the agreement is considered to be good. It was obtained that the highest %Error between S-K, R-K and 3-D elasticity is less than %2.

5. Conclusions

A single layer shear deformation plate theory with superposed shape functions for laminated composite structures has been proposed by using combinations of some previously proposed higher order shear deformation theories (parabolic [1], trigonometric [2], exponential [3] and trigonometric [4] shear deformation plate theories). Some statics and dynamics composite plate problems have been investigated. The obtained results are compared with the 3-D elasticity solutions. It was determined that superposed theories provide some improvements for the $y - z$ component of the transverse shear stress and approximately gives similar results for other stress and bending values. In general, R-K and S-K models have lower errors when compared to other models considered. It was concluded that using different shear functions in the displacement field in different in-plane directions may improve the effectiveness of the shear deformable theories. Extension of this study can be considered for other boundary conditions and lamination configurations.

References

1. J.N. Reddy, *A simple higher-order theory for laminated composite plates*, Journal of Applied Mechanics, **51**, 745–752,1984.

2. K.P. Soldatos, *A transverse shear deformation theory for homogeneous monoclinic plates*, Acta Mechanica, **94**, 1995–220,1992.

3. M. Karama, K.S. Afaq, S. Mistou, *Mechanical behavior of laminated composite beam by new multi-layered laminated composite structures model with transverse shear stress continuity*, International Journal of Solids and Structures, **40**, 1525–1546, 2003.

4. C.H. Thai, A.J.M. Ferreira, S.P.A. Bordos, T. Rabczuk, H. Nguyen-Xuan, *Isogeometric analysis of laminated composite and sandwich plates using a new inverse trigonometric shear deformation theory*, European Journal of Mechanics A- Solids, **43**, 89–108, 2014.

5. R.D. Mindlin, *Influence of rotary inertia and shear on flexural motions of isotropic elastic plates*, Journal of Applied Mechanics, **18**, A31–A38, 1951.

6. E. Reissner, *On transverse bending of plates including the effects of transverse sheart deformation*, International Journal of Solids and Structures, **25**, 495–502, 1975.

7. S.A. Ambartsumian, *On the theory of bending plates*, Series of the Academy of Sciences of the Soviet Union, **5**, 69–77, 1958 [in Russian].

8. M. Troutier, *An efficient standard plate theory*, International Journal of Engineering Sciences, 29, **8**, 901–916, 1991.

9. M. Aydogdu, *A new shear deformation theory for laminated composite plates*, Composite Structures, **89**, 94–101, 2009.

10. J.L. Mantari, A.S. Oktem, C.G. Soares, *A new trigonometric shear deformation theory for isotropic, laminated composite and sandwich plates*, International Journal of Solids and Structures, **49**, 1, 43–53, 2012.

11. T. Timarci, K.P. Soldatos, *Comparative dynamic studies for symmetrical cross-ply circular cylindrical shells on the basis of a unified shear-deformable shell theory*, Journal of Sound and Vibration, **187**, 4, 609–624, 1995.

12. M. Aydogdu, T. Timarci, *Vibration analysis of cross-ply laminated square plates with general boundary conditions*, Composites Science and Technology, **63**, 7, 1061–1070, 2003.

13. M. Aydogdu, *Comparison of various shear deformation theories for bending, buckling and vibration of rectangular symmetric cross-ply plate with simply supported edges*, Journal of Composite Materials, **40**, 23, 2143–2155, 2006.

14. C.P. Wu, W.Y. Chen, *Vibration and stability of laminated plates based on a local high order plate theory*, Journal of Sound Vibration, **177**, 4, 503–520, 1994.

15. K.N. Cho, C.W. Bert, A.G. Striz, *Free vibrations of laminated rectangular plates analysed by higher order individual-layer theory*, Journal of Sound and Vibration, **145**, 3, 429–442, 1991.

16. S. Abrate, M. Di Sciuva, *Equivalent single layer theories for composite and sandwich structures: a review*, Composite Structures, **179**, 482–494, 2017.

17. T. Timarci, M. Aydogdu, *Buckling of symmetric cross-ply square plates with various boundary conditions*, Composite Structures, **68**, 4, 381–389, 2017.

18. C.T. Herakovich, *Mechanics of Composite Materials*, McGraw-Hill, New York, 1998.

19. H.L. Langhaar, *Energy Methods in Applied Mechanics*, John Wiley and Sons, 1962.

20. J.M. Whitney, *Structural Analysis of Laminated Plates*, Technomic, Lancaster, 1987.

21. N.J. Pagano, S.J. Hatfield, *Elastic behaviour of multilayered bidirectional composites*, American Institute of Aeronautics and Astronautics Journal, **10**, 931–933, 1972.

22. N.J. Pagano, *Exact solutions for rectangular bidirectional composites and sandwich plates*, Journal of Composite Materials, **4**, 21–35, 1970.

23. A.K. Noor, *Free vibrations of multilayered composite plates*, American Institute of Aeronautics and Astronautics Journal, **11**, 7, 1038–1039, 1972.

24. N.D. Phan, J.N. Reddy, *Analyses of laminated composite plates using a higher-order deformation theory*, International Journal for Numerical Methods in Engineering, **21**, 2201–2219, 1985.

25. A.K Noor, *Stability of multilayered composite plates*, Fibre Science Technology, **8**, 2, 81–89, 1975.